

Original Article

Inflammation reduction potential of nanostructured lipid carriers encapsulated with rat's bone marrow cells' lysate

Potencial de redução da inflamação de carreadores lipídicos nanoestruturados encapsulados com lisado de células de medula óssea de ratos

S. Malik^a , S. J. Awan^{a,b*} , A. Farzand^a  and Q. Ali^c 

^aThe University of Lahore, Institute of Molecular Biology and Biotechnology – IMBB, Lahore, Pakistan

^bKinnaird College For Women, Department of Zoology, Lahore, Pakistan

^cUniversity of the Punjab, Department of Plant Breeding and Genetics, Lahore, Pakistan

Abstract

Bone marrow-derived mesenchymal stromal cells (BMSCs) have been used for treating inflammatory disorders. Due to the large size of BMSCs compared to nanoparticles, BMSCs cannot be loaded into the nanoparticles. It is hypothesized that BMSCs lysate loading into the nanocarriers will effectively deliver cellular contents and regulatory elements of BMSCs at the injury site. This study aimed to investigate nanostructured lipid carriers (NLC) loading with BMSCs lysate through basic characterization and morphological analysis. Moreover, this study was mainly designed to investigate the role of NLC loaded BMSCs lysate in reducing inflammation via *in-vitro* and *in-vivo* assays. The *in-vitro* study involves cell viability assays, p53, annexin V and VEGF expression through ELISA and immunocytochemistry, real-time BAX, caspase-3, IL-6, IL-8, TOP2A, PCNA, and Ki-67 gene expression analysis. Additionally, to evaluate *in-vivo* anti-inflammatory activity, the carrageenan-induced rat paw oedema model was used. *In-vitro* results showed that NLC loaded BMSCs lysate increased cell viability, decreased apoptosis and pro-inflammatory genes expression and up-regulated angiogenesis and proliferation in H₂O₂ pre-stimulated cells. Findings of the *in-vivo* assay also indicated a reduction in rat's paw oedema volume in NLC-loaded BMSCs lysate, and downregulation of BAX, Caspase-3, IL-6, and IL-8 was observed. Enhanced expressions of TOP2A, PCNA, and Ki-67 were obtained. Concluding the results of this study, NLC-loaded BMSCs lysate could reduce inflammation and possibly regenerate damaged tissue mainly via increasing cell viability, angiogenesis and proliferation, and reducing apoptosis and pro-inflammatory cytokines.

Keywords: lysate, nanostructured lipid carriers, bone marrow-derived mesenchymal stromal cells, anti-inflammatory activity, carrageenan-induced rat paw oedema.

Resumo

Células estromais mesenquimais derivadas da medula óssea (BMSCs) têm sido utilizadas para o tratamento de distúrbios inflamatórios. Devido ao grande tamanho das BMSCs em comparação com as nanopartículas, as BMSCs não podem ser carregadas nas nanopartículas. Supõe-se que o carregamento de lisado de BMSCs no nanocarriers será eficaz na entrega de conteúdos celulares e elementos reguladores de BMSCs no local da lesão. Este estudo teve como objetivo investigar a carga de carreador lipídico nanoestruturado (NLC) com lisado de BMSCs através de caracterização básica e análise morfológica. Além disso, este trabalho foi projetado, principalmente, para investigar o papel do lisado de BMSCs carregado com NLC na redução da inflamação por meio de ensaios anti-inflamatórios *in vitro* e *in vivo*. O estudo *in vitro* envolve ensaios de viabilidade celular, expressão de p53, anexina V e VEGF por ELISA e imunocitoquímica e expressão gênica em tempo real de BAX, caspase-3, IL-6, IL-8, TOP2A, PCNA e Ki-67. Além disso, para avaliar a atividade anti-inflamatória *in vivo*, o modelo de edema de pata de rato induzido por carragenina foi utilizado. Os resultados *in vitro* mostraram que o lisado de BMSCs carregadas com NLC aumentou a viabilidade celular, diminuiu a apoptose e a expressão de genes pró-inflamatórios e aumentou a angiogênese e proliferação em células pré-estimuladas com H₂O₂. Os achados do ensaio *in vivo* também indicaram uma redução no volume do edema da pata de rato no lisado de BMSCs carregado com NLC, entretanto, foi observada a regulação negativa de BAX, Caspase-3, IL-6 e IL-8. Expressões aumentadas de TOP2A, PCNA e Ki-67 foram obtidas. Assim, concluindo os resultados do estudo, é possível afirmar que o lisado de BMSCs carregado com NLC pode reduzir a inflamação e possivelmente regenerar o tecido danificado principalmente por meio do aumento da viabilidade celular, angiogênese e proliferação e redução da apoptose e citocinas pró-inflamatórias.

Palavras-chave: lisado, transportador lipídico nanoestruturado, células estromais mesenquimais derivadas da medula óssea, atividade anti-inflamatória, edema de pata de rato induzido por carragenina.

*e-mail: sana.javaidawan@yahoo.com; sana.javaid@kinnaird.edu.pk; saim1692@gmail.com

Received: November 15, 2022 – Accepted: December 1, 2022



This is an Open Access article distributed under the terms of the Creative Commons Attribution License, which permits unrestricted use, distribution, and reproduction in any medium, provided the original work is properly cited.

1. Introduction

Inflammation is a complex, dynamic, and natural body response against harmful infection (Aghasafari et al., 2019) that may lead to cancer, autoimmune diseases, or neurodegenerative disorders if it remains unchecked (Hossen et al., 2017). The prevention of the upregulation of inflammation reactions could help prevent many life-threatening disorders (Furman et al., 2019).

Bone marrow-derived mesenchymal stromal cells (BMSCs) are progenitor cells that have gained much attention in regenerative medicines (Mohanty et al., 2020). Nanostructured lipid carriers (NLC) are the latest advancement of lipid-based particles possessing increased water solubility of drugs, enhanced drug enclosing potential, increased durability to carry an additional quantity of the drug, and minimized drainage of the drug (Ferreira et al., 2021).

The approximate size of mesenchymal stromal cells (MSCs) is 17-30 μm (Ge et al., 2014), while the average size of solid-lipid-based nanoparticles is 10-400 nm (Yoon et al., 2013). Due to the larger size of MSCs compared to nanoparticles, they cannot be loaded into the nanoparticles. It is hypothesized that BMSCs lysate loading into the nanocarriers would effectively deliver cellular contents to the injury site. The use of cell lysate could be an effective cell-free treatment for different diseases. Without direct contact of live cells on the host tissue, the treatment of cell lysate exposes the tissue to various soluble components present in MSCs, e.g., growth factors, cytokines, and microvesicles holding micro RNAs (Malik and Malik, 2021; Yeghiazarians et al., 2009; Malik et al., 2021; Zafar et al., 2022; Afzal et al., 2022; Noor et al., 2022; Butt et al., 2022). The study aimed to investigate the loading of NLC with BMSCs lysate and its role in reducing inflammation *in-vitro* and *in-vivo* for the first time.

2. Materials and Methods

2.1. Animals and their maintenance

In this study, healthy *Sprague dawley* rats were housed in the standard living environment. All experimental procedures complied with the Guide for the care and use of laboratory animals by the USA National Institutes of Health (NIH publication number 85-23). More details have been provided in the supplementary material.

2.2. Cell culture: culturing of BMSCs and BMSCs lysate preparation

BMSCs were obtained from the bone marrow of *Sprague dawley* rats (weighing 90-150 g) following the method narrated by Sharif et al. (2007) (See supplementary material for more details).

2.3. Preparation of Nanostructured Lipid Carriers (NLC) and NLC-loaded BMSCs lysate

NLC was prepared by a nanotemplate engineering technique used by Kim et al. (2012), making minor changes Arshad et al. (2019). (See supplementary material for more details).

2.4. Basic characterization and morphological analysis of NLC and NLC-loaded BMSCs lysate

The particle size analysis and zeta-potential, scanning electron microscopy (SEM), and enzyme-linked immunosorbent assay (ELISA) were utilized for the basic characterization of NLC and NLC-loaded BMSCs lysate. (See supplementary material for more details).

2.5. In-vitro anti-inflammation assay

2.5.1. Culturing of cell line

NIH 3T3 (mouse fibroblast) cell line was cultured in DMEM-HG (enriched with NaHCO_3 (3.7 g/L), streptomycin (1%), FBS (10%), and penicillin (0.1%)). Cells were placed in an incubator at 37 °C with 5% CO_2 and were used in subsequent experiments (See supplementary material for more details).

2.6. Experimental design

The NIH 3T3 cell line at the 2nd passage was cultured into Thermo Fisher 96-micro well culture plates to evaluate the MTT cell viability assay. When NIH 3T3 cells achieved 80% confluency, they were given injury with IC_{50} (6.625 mM) of H_2O_2 for two hours. After two hours, these H_2O_2 pre-stimulated cells were exposed to different concentrations of NLC, BMSCs lysate, and NLC-loaded BMSCs lysate for 24 hours. NIH 3T3 cells were grouped into four categories (see Table 1). Upon incubation for 24 hours, secretome (used medium of cells) was used for enzyme-linked immunosorbent assay (ELISA) and antioxidants. Cells of NIH 3T3 were grown in 24-microwell culture plates, which were used for RNA isolation and immunocytochemistry experiments.

Table 1. *In-vitro* anti-inflammatory experimental groups.

NIH 3T3 Treatment Groups	Description
Untreated Cells (UT)	NIH 3T3 cells without any treatment
H_2O_2 Injury group (I- H_2O_2)	NIH 3T3 cells pre-stimulated with H_2O_2
Treated nanostructured lipid carriers group (T-NLC)	H_2O_2 pre-stimulated NIH 3T3 cells treated with NLC
Treated BMSCs lysate group (T-BMSCs-L)	H_2O_2 pre-stimulated NIH 3T3 cells treated with BMSCs lysate
Treated NLC loaded BMSCs lysate group (T-NLC-BMSCs-L)	H_2O_2 pre-stimulated NIH 3T3 cells treated with NLC loaded BMSCs lysate

2.7. In-vitro post-treatment evaluation

2.7.1. MTT cell viability assay

This assay was applied to detect the proliferative potential of various concentrations (500µg/µL, 1mg/mL, 2mg/mL, 3mg/mL) of two treatments, *i.e.*, NLC, BMSCs lysate, and NLC-loaded BMSCs lysate after injury with H₂O₂ and further calculations of standardized viability calculations (SVC). After H₂O₂ injury, as mentioned above, 100µL of different treatments were given. After 24 hours, the MTT assay was performed following the procedure mentioned by Awan et al. (2017). The percentage of cell viability was derived by using the following Formula 1:

$$\%viability = (SampleODat570nm \div ControlODat570nm) \times 100 \quad (1)$$

For all subsequent experiments, the SVC value of each group was used.

2.8. Enzyme-linked immunosorbent assay (ELISA)

For the expression of secretory proteins in a conditioned medium of different groups, solid-phase sandwich ELISA was used following the methodology of Wajid et al.(2015) for p53, annexin V, and VEGF. (See supplementary material for more details).

2.9. Immunocytochemistry

Immunocytochemistry was also carried out following the procedure explained by Wajid et al. (2013) on NIH 3T3 cells of different treatment groups. The primary antibodies (Santa Cruz Biotechnology, USA product line) were rabbit polyclonal anti-p53, anti-annexin V and anti-VEGF. In contrast, the secondary antibody was tetramethylrhodamine (TRITC) tagged donkey anti-rabbit (Santa Cruz Biotechnology, USA). Fluorescent dye 4',6-diamidino-2'-phenylindole dihydrochloride (DAPI) was used to stain nuclei.

2.10. In-vitro gene expression profiling

For the post-treatment *in-vitro* gene expression analysis, RNA was isolated from all NIH 3T3 cells group, followed by real-time (qPCR) PCR. It was done using the SYBR Green dye-containing PCR SuperMix (Fermentas, USA) on the iQ5 real-time PCR detection system (Bio-Rad,

USA). In *in-vitro* experimental groups, expression levels of apoptotic (BAX and Caspase-3) markers, proliferative (Ki-67, PCNA, and TOP2A) markers, and inflammatory markers (IL-6 and IL-8) were checked while GAPDH served as an internal control measure.

2.11. In-vivo anti-inflammatory activity

2.11.1. Carrageenan-induced rat paw oedema

To check the effect of lysate on reducing inflammation/oedema, carrageenan was injected into the hind paw to induce oedema following the procedures by Winter et al.(1962). Rats were divided into seven groups, as shown in Table 2.

2.12. Treatment of paw oedema

BMSCs lysate and BMSCs lysate loaded NLC were administered to the rats to treat and check their anti-inflammatory activity. After 1 hour of carrageenan injection, different treatments, *i.e.*, normal saline, diclofenac sodium (DFS), NLC (2mg/kg of rat body weight), BMSCs-L (2mg/kg of rat body weight), and NLC-BMSCs-L (2mg/kg of rat body weight) were injected. An anti-inflammatory drug (DFS) was applied in this study as a standard drug. Rats receiving normal saline through injection were part of the vehicle control group. The swelling of carrageenan injected foot and treated groups was measured at different hours using a plethysmometer. Percent inhibition of inflammation of test samples was calculated in comparison with vehicle control by using the following Formula 2:

$$\% inhibition = 100(1 - Vt / Vc) \quad (2)$$

where Vc represents oedema volume in control and Vt the oedema volume in the group treated" (Su et al., 2011).

2.13. In-vivo post-treatment evaluation

After 24 hours of treatment, all the experimental group rats were sacrificed, and their paw tissue was taken for RNA isolation using aTRIZOL reagent.

2.14. In-vivo gene expression profiling

For *in-vivo* gene expression analysis, qPCR was executed as mentioned above.

Table 2. In-vivo anti-inflammatory experimental groups.

Experimental Groups	Description
Control group (N)	Normal rats
Vehicle Control Group (N-NS)	Normal rats saline-injected
Carrageenan Injury Group (C)	Carrageenan induced rats without any treatment
Carrageenan Induced Normal Saline (C-NS)	Carrageenan-induced rats injected with normal saline
Positive control (C-I-DFS)	Carrageenan-induced rats injected with standard drug diclofenac sodium(DFS)
Carrageenan induced NLC (C-I-NLC)	Carrageenan-induced rats injected with NLC
Carrageenan-induced BMSCs lysate (C-I-BMSCs-L)	Carrageenan-induced rats injected with BMSCs-L
Carrageenan induced NLC loaded BMSCs lysate (C-I-NLC-BMSCs-L)	Carrageenan-induced rats injected with NLC loaded BMSCs lysate

2.15. Statistical analysis

Unless otherwise mentioned, data are shown as mean values ± SEM. For comparison of more than two datasets, the one-way analysis of variance (ANOVA) and grouped datasets, the two-way ANOVA was done using the Bonferroni posttest. All statistical analyses of the results were performed through Prism v.5, GraphPad software (USA). P values <0.05 were regarded as statistically significant, and non-significant differences were indicated.

3. Results

3.1. NLC preparation and basic characterization

Zeta size analysis and SEM were performed to characterize NLC and NLC loaded BMSCs lysate. Zeta size analysis (see Table 3) and SEM (see Figure 1A, B) showed the synthesised particles' size, polydispersity index, and surface morphology. The particles of NLC with a Z-average size of 20.15 nm and NLC-BMSCs-L with a Z-average size of 21.73 nm appeared to be slightly smooth (size distribution curve has been provided in the supplementary material). ELISA was performed to investigate the loading of BMSCs lysate inside the NLC. VEGF and IL-6 marker's expression was checked in NLC, BMSCs lysate, and NLC-BMSCs-L groups. The results in Figure 1B shows that VEGF and IL-6 levels are detected in NLC-loaded BMSCs lysate, which confirms the loading of BMSCs lysate in NLC while no expression was observed in NLC.

3.2. In vitro anti-inflammation assay results

3.2.1. Decreased cytotoxicity of post-treated NIH 3T3 cells

To induce *in-vitro* inflammation in NIH 3T3 cells via H₂O₂, 6.625 mM H₂O₂ was used in experiments to induce

in-vitro injury and evoke inflammation *in-vitro*. To calculate the standardized viability concentration (SVC), an MTT assay was performed using different concentrations of NLC, BMSCs lysate, and NLC-loaded BMSCs lysate. In this experiment, SVC defines the concentration at which the cells show 100% viability. The MTT cytotoxicity assay showed that BMSCs lysate and NLC-loaded BMSCs lysate had a dose-dependent effect on NIH 3T3 cell growth (see Figure 2). As represented in Figure 3, after injury with H₂O₂, NIH 3T3 cells treated with BMSCs lysate at the concentration level of 1.61 mg/mL for 24 hours of treatment showed 100% cell viability. NLC-loaded BMSCs lysate showed 100% viable cells at a concentration of 1.42 mg/mL. These SVC values were applied in subsequent experiments. While NLC was used at a concentration of 1.42 mg/mL in later experiments.

3.3. Inflation of angiogenesis in post-treated NIH 3T3 cells

Further, to assess the effect of two different treatments, *i.e.*, BMSCs lysate and NLC-loaded BMSCs lysate, on angiogenesis, vascular endothelial growth factor (VEGF) levels were assessed via ELISA and immunocytochemistry in NIH 3T3 cells after exposure with these treatments, as VEGF is the principal factor behind angiogenesis. Figures 3A and 4A indicate a significant VEGF expression elevation in the NLC-loaded BMSCs lysate group compared to the H₂O₂ injury and BMSCs lysate groups.

3.4. Apoptosis reduction in post-treated NIH 3T3 cells

To determine whether NLC-loaded BMSCs lysate has an anti-apoptotic effect on NIH 3T3 cells, apoptosis levels were measured via p53 and annexin V expression studies through ELISA and immunocytochemistry. The results of these assays manifest (see Figures 3B and 4B, C) that its

Table 3. Physiochemical Characteristics of NLC and NLC-BMSCs-L.

Formulation	Z-Average Size (d.nm)	Polydispersity Index (PDI)	PDI Width (d.nm)	Peak Mean/Area (d.nm/%)	Zeta Potential
NLC	20.15	0.101	6.412	13.43/100	±8.310
NLC-BMSCs-L	21.73	0.134	7.951	12.55/100	±8.222

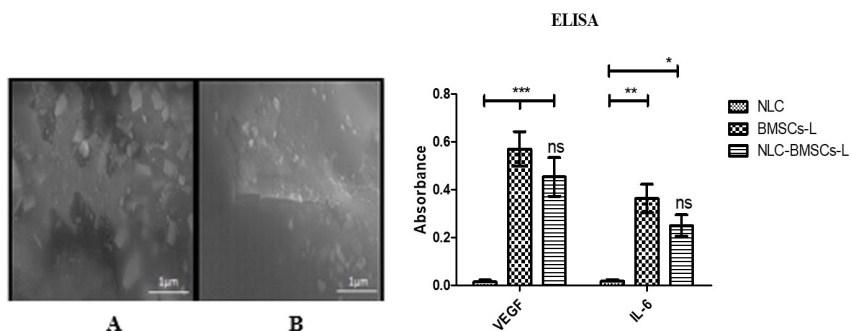


Figure 1. (A) Scanning Electron Micrograph of NLC and (B) Scanning Electron Micrograph of NLC-BMSCs-L; (C) Characterization of nanostructured lipid carriers (NLC) loaded bone marrow-derived mesenchymal stromal cells (BMSCs) lysate via enzyme-linked immunosorbent assay (ELISA):vascular endothelial growth factor (VEGF) and interleukin-6 (IL-6) expression in NLC, BMSCs-L, and NLC loaded bone marrow-derived mesenchymal stromal cells lysate (NLC-BMSCs-L). Where; *P<0.05, **P<0.01, ***P<0.0001, ns is non-significant.

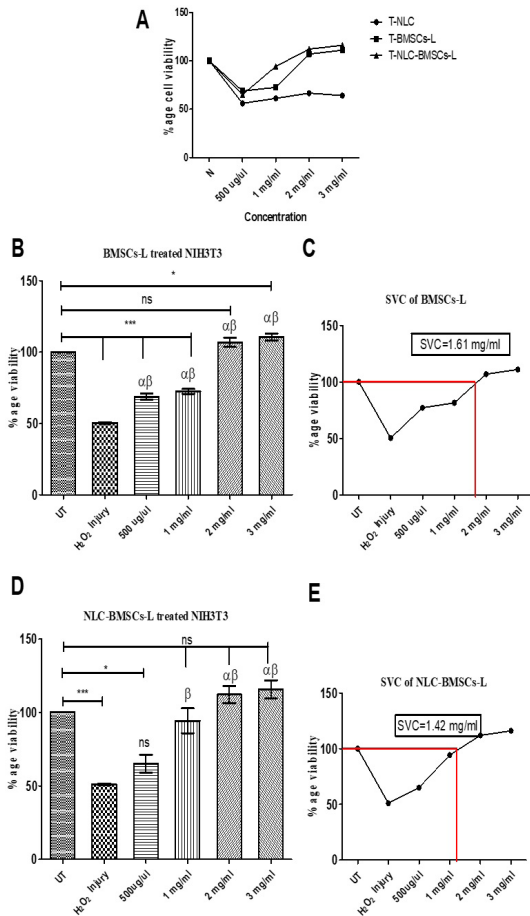


Figure 2. Represents cytotoxicity analysis/percentage cell viability and standardized viability concentration (SVC) values of different treatment groups on NIH 3T3 Cells (A) Represents the percentage of NIH 3T3 cells viability treated with different concentrations of nanostructured lipid carriers (NLC), bone marrow-derived mesenchymal stromal cells lysate (BMSCs-L), and NLC loaded BMSCs lysate (NLC-BMSCs-L). N represents % age viability of normal cells that receive no treatment and no H₂O₂ injury; (B) Cytotoxicity analysis of various concentrations (500µg/µL, 1mg/mL, 2mg/mL, and 3mg/mL) of BMSCs lysate (C) SVC of BMSCslysate on NIH 3T3 cells; (D) Cytotoxicity analysis of various concentrations (500µg/µL, 1mg/mL, 2mg/mL, and 3mg/mL) of NLC loaded BMSCs lysate (E) shows SVC of NLC loaded BMSCs lysate on cells. Where; ***P<0.0001, *shows significance between untreated and treated groups while α and β sign shows significance between H₂O₂ injury and other treatment groups, $\alpha\beta$ shows P<0.0001, and ns is non-significant.

expression significantly declines in NLC loaded BMSCs lysate group when compared to injury, NLC and BMSCs lysate groups.

3.5. Modulation of in-vitro gene expression in post-treated NIH 3T3 cells

To check the effect of NLC-loaded BMSCs lysate at the molecular level of apoptosis, inflammation, and proliferation, investigation of apoptotic, pro-inflammatory,

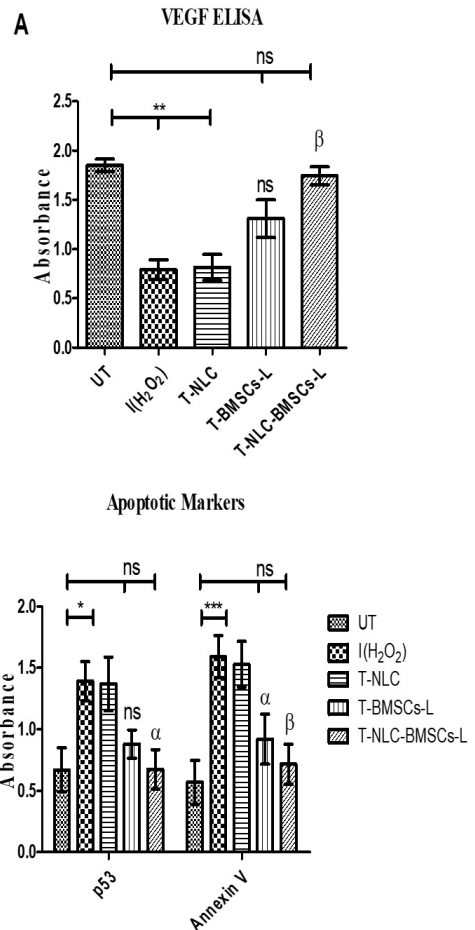


Figure 3. (A) Angiogenesis Expression Analysis via ELISA:vascular endothelial growth factor (VEGF) expression in treated BMSCs lysate group (T-BMSCs-L) and treated NLC loaded bone marrow-derived mesenchymal stromal cells lysate (T-NLC-BMSCs-L) group as compared to untreated (UT), treated NLC (T-NLC), and H₂O₂ injury (I-H₂O₂) groups; (B) Apoptosis Expression Analysis via ELISA. The level of apoptosis measured via p53 and annexin V markers is indicated in different treatment groups. While the * sign shows significance between untreated and treated groups while α and β sign shows significance between H₂O₂ injury and other treatment groups, where; ns is non-significant, * & α signify P<0.05, ** & β signify P<0.01, *** & $\alpha\beta$ signify P<0.001.

and proliferative gene expression analysis was carried out in pre and post-treated NIH 3T3 cells. qPCR results demonstrated that, in H₂O₂ induced injury group, the level of apoptotic genes (BAX and Caspase-3, see Figure 5A and pro-inflammatory cytokines (interleukin-6 (IL-6) and interleukin-8 (IL-8), see Figure 5B significantly increased whereas, the level of proliferative genes (Ki-67, PCNA, TOP2A, see Figure 5C) decreased. In the NLC-loaded BMSCs lysate group, significant downregulation of apoptotic (see Figure 5A) and pro-inflammatory genes (see Figure 5B), while upregulation of proliferative genes (see Figure 5C) was observed compared to BMSCs lysate. GAPDH served as an internal control.

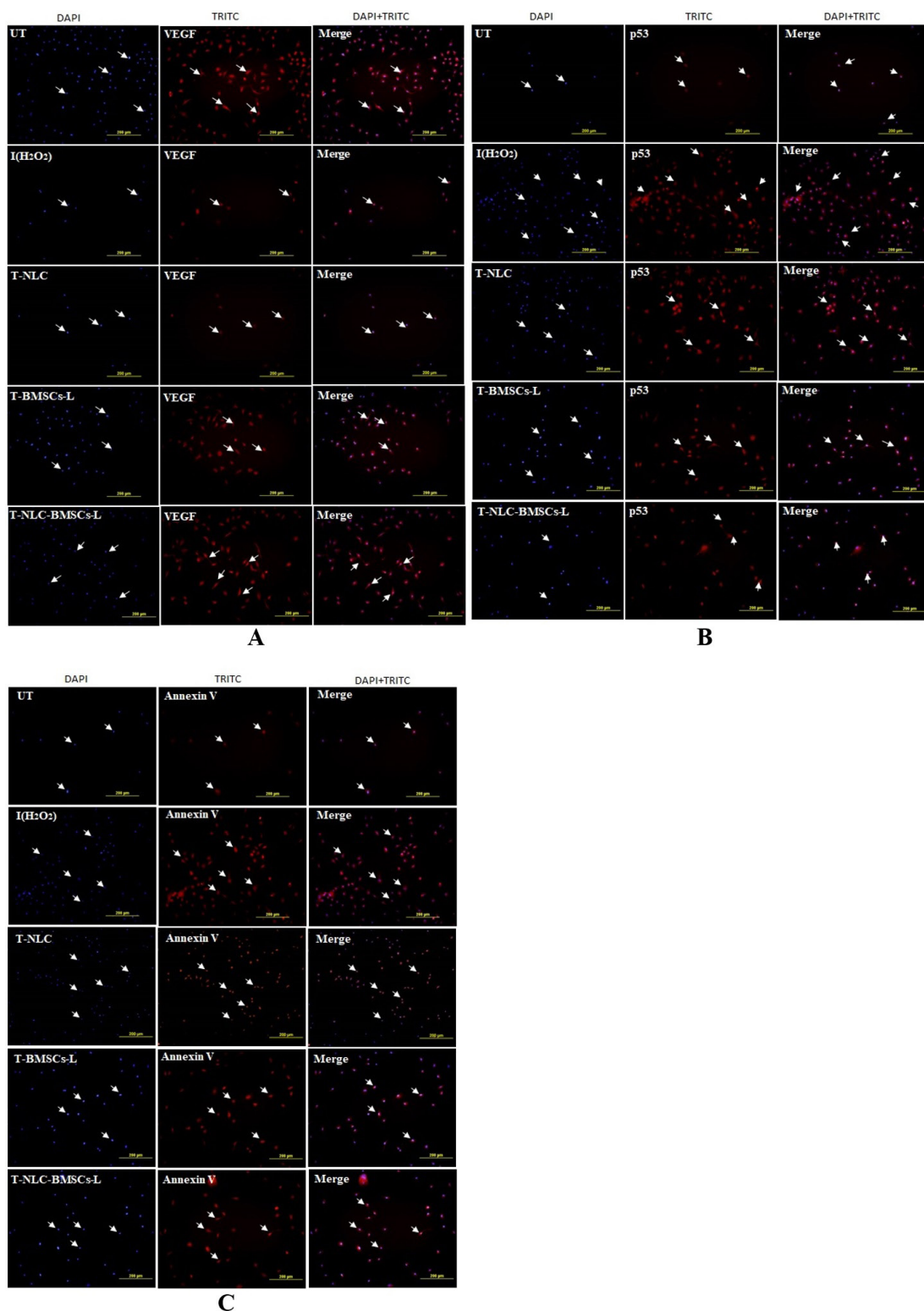


Figure 4. (A) Expression analysis of angiogenesis marker vascular endothelial growth factor (VEGF) via immunocytochemistry; (B) Expression analysis of apoptotic marker p53 via immunocytochemistry; (C) Expression analysis of apoptotic marker p53 via immunocytochemistry. Where: Untreated (UT), H₂O₂ injury (I-H₂O₂), treated NLC (T-NLC), treated BMSCs lysate (T-BMSCs-L), and treated NLC loaded bone marrow-derived mesenchymal stromal cells lysate (T-NLC-BMSCs-L). Stained cells are red, and blue denotes the nuclei counterstained with 4',6-diamidine-2'-phenylindole dihydrochloride (DAPI,) while arrows show the positive cells expressing the protein. Scale bar: 200μm.

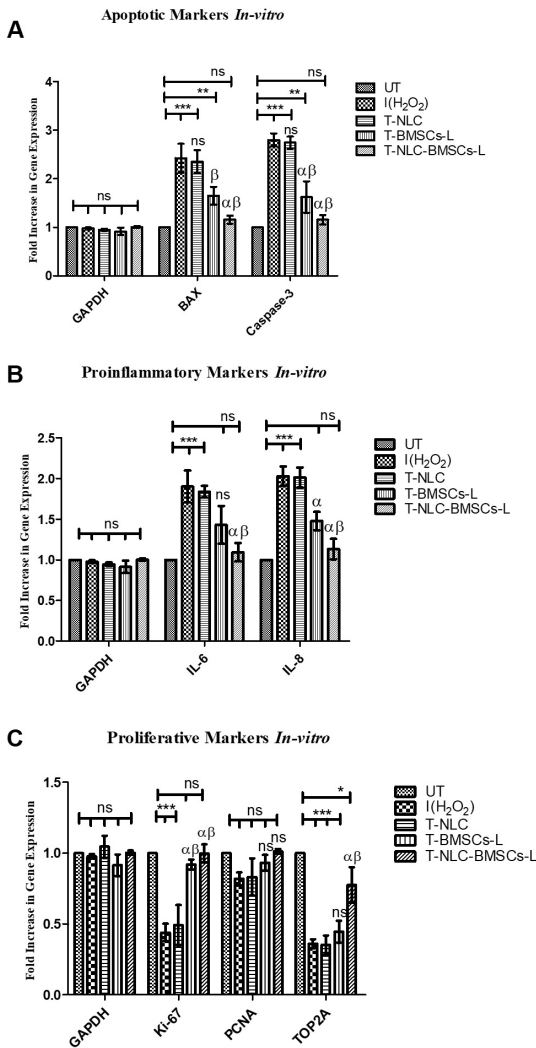


Figure 5. *In-vitro* Gene Expression Analysis: (A) represents apoptotic markers; BAX & Caspase-3, expression among treated nanostructured lipid carriers (T-NLC), treated bone marrow-derived mesenchymal stromal cells (BMSCs) lysate (T-BMSCs-L) and NLC loaded BMSCs lysate (T-NLC-BMSCs-L) groups as compared to untreated (UT), and H₂O₂ injury (I-H₂O₂) groups (B) shows pro-inflammatory markers (IL-6 and IL-8) expression in T-NLC-BMSCs-L group as compared to I-H₂O₂ group (C) shows Proliferative markers (Ki-67, PCNA and TOP2A) expression among T-BMSCs-L and T-NLC-BMSCs-L groups as compared to UT and I-H₂O₂ group. Where; * sign shows significance between untreated and treated groups while α and β sign shows significance between H₂O₂ injury and other treatment groups. Where; ns is non-significant, * & α implies P<0.05, ** & β implies P<0.001, *** & $\alpha\beta$ implies P<0.0001.

3.6. *In-vivo* anti-inflammation assay results

3.6.1. Reduction of rat paw oedema volume after treatment

A carrageenan-induced rat hind paw oedema assay was performed to evaluate further the NLC-loaded BMSCs lysate anti-inflammatory potential. The anti-inflammatory potential of two experimental groups, i.e., BMSCs lysate and

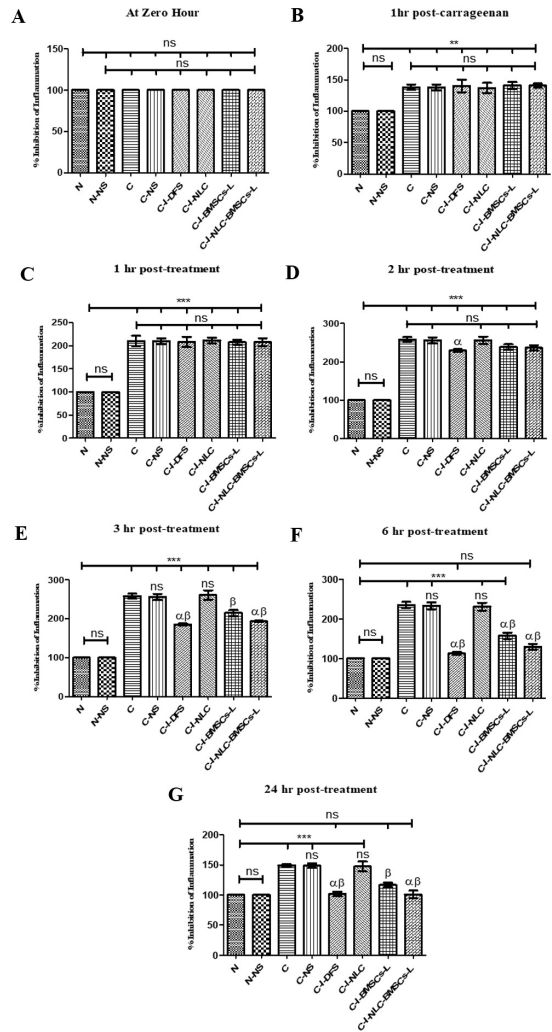


Figure 6. Percentage inhibition of inflammation at a time interval (hr) in carrageenan-induced rat's hind paw oedema model. The effect of different treatment groups, i.e., normal (N), normal rat paw injected with normal saline (N-NS), carrageenan injected group (C), carrageenan injected with normal saline group (C-NS), carrageenan injected with diclofenac sodium group (C-I-DFS), carrageenan injected with nanostructured lipid carriers group (C-I-NLC), carrageenan injected with bone marrow-derived mesenchymal stromal cells (BMSCs) lysate group (C-I-BMSCs-L) and Carrageenan injected with NLC loaded BMSCs lysate group (C-I-NLC-BMSCs-L); on hind paw oedema at different hours (0, 1, 2, 3, 6 & 24 hours). Where; the * sign shows significance between normal and carrageenan-induced treated groups while α and β sign shows significance between carrageenan injected and carrageenan-induced treatment groups. Where; ns is non-significant, ** & β denotes P<0.001, *** & $\alpha\beta$ denotes P<0.0001.

NLC-loaded BMSCs lysate and the percentage inhibition of inflammation at a time interval (hr), are shown in Figure 6. In nearly all treated groups, carrageenan-induced rat paw oedema reached a maximum after 3 hours of injection and started to decline after that. The results of this assay revealed that NLC-loaded BMSCs lysate exhibits strong anti-inflammatory potential compared to BMSCs lysate

group against acute inflammation. The experimental groups possessed less inflammation than the carrageenan and vehicle control groups and were comparable to the positive standard group. The percentage inhibition of inflammation after 24 hours of control and treated groups was not significantly different (see Figure 6)(Paw images have been provided in the supplementary material).

3.7. In-vivo modulation of gene expression

Next, qPCR was done to investigate the effect of experimental groups on in-vivo gene expression profiling pro-inflammatory cytokines, apoptosis, and proliferation genes. Results revealed that NLC-loaded BMSCs lysate significantly decreases carrageenan-induced upregulation of pro-inflammatory cytokines, IL-6 and IL-8, and apoptotic markers; BAX and caspase-3 compared to other groups (see Figures 7A, B). While NLC-loaded BMSCs lysate significantly up-regulates the expression of proliferative markers, Ki-67, PCNA, and TOP2A as compared to the BMSCs lysate group (see Figures 7C). Glyceraldehyde-3-phosphate dehydrogenase, abbreviated as GAPDH, served as an internal control measure.

4. Discussion

With the formulated formulation and by using the Nano-template engineering technique, the nano-sized particles were obtained as formerly narrated (Arshad et al., 2019). Basic characteristics of resulting NLC, such as Z-average size and polydispersity index (see Table 3), showed the average size of NLC loaded BMSCs lysate being marginally higher than the unloaded NLC due to the integration of lysate in the NLC matrix, which is in accordance with Hu et al. (2005). Moreover, to further confirm the loading of BMSCs lysate in NLC, the expression of VEGF and IL-6 proteins was assessed via ELISA in NLC, BMSCs lysate, and NLC-loaded BMSCs lysate groups. The results indicated that VEGF and IL-6 expressions were detected inside the NLC-loaded BMSCs lysate group.

To find out the standardized viability concentration (SVC), the same concentrations (500µg/µL, 1mg/mL, 2mg/mL, 3mg/mL) of BMSCs lysate and NLC loaded BMSCs lysate were used to find out the individual effect of each on cell viability of H₂O₂ pre-stimulated cells. SVC for BMSCs lysate was calculated at a concentration of 1.61mg/mL and for NLC-loaded BMSCs lysate was obtained at 1.42mg/mL (see Figure 2). These SVC values were used in subsequent experiments. This also shows that the loading of lysate in NLC significantly enhances the efficacy of lysate.

VEGF is a well-known key element of angiogenesis (Moccia et al., 2019) that plays a crucial role in mediating vascular permeability and tissue regeneration (Masgutov et al., 2021). Based on ELISA and immunocytochemistry assay results (see Figures 3A and 4A), there was a decrease in the expression pattern of VEGF in H₂O₂ pre-stimulated NIH 3T3. In contrast, an increase in its expression was significantly observed in the post-treated cells in the NLC-loaded BMSCs lysate group compared to BMSCs lysate alone.

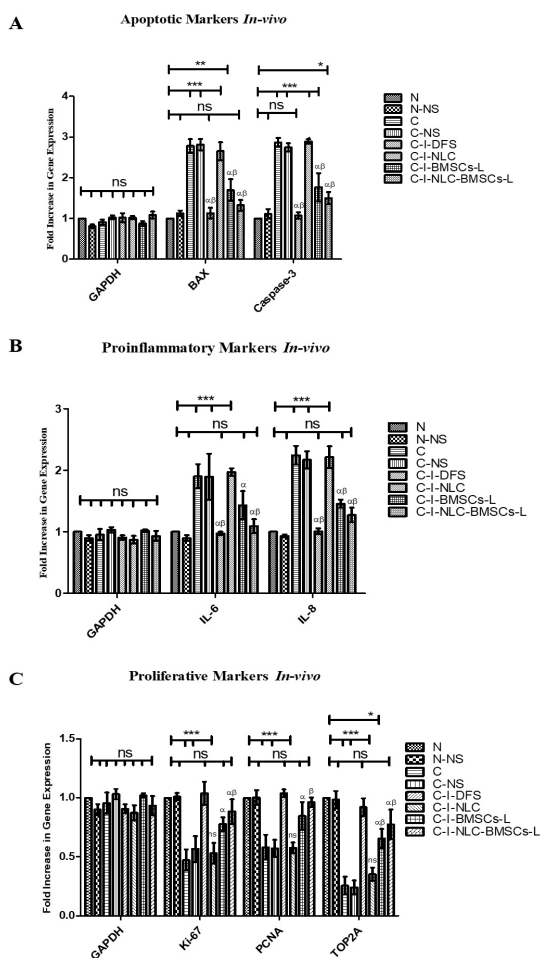


Figure 7. In-vivo Gene Expression Analysis: (A) represents apoptotic markers; BAX and Caspase-3, expression in treated nanostructured lipid carriers (T-NLC), treated bone marrow-derived mesenchymal stromal cells (BMSCs) lysate (C-I-BMSCs-L) and NLC loaded BMSCs lysate (C-I-NLC-BMSCs-L) groups as compared to normal (N) and carrageenan injected injury (C) groups (B) shows pro-inflammatory markers (IL-6 and IL-8) expression levels in treated C-I-BMSCs-L and treated C-I-NLC-BMSCs-L groups as compared to N and C groups (C) shows Proliferative markers (Ki-67, PCNA and TOP2A) expression in treated C-I-BMSCs-L and treated C-I-NLC-BMSCs-L group as compared to N and C groups. Whereas N-NS represents normal rats injected with normal saline, C-NS represents carrageenan-injected normal saline, C-I-DFS represents carrageenan-injected diclofenac sodium. Where; the* sign shows significance between untreated and treated groups while α and β sign shows significance between carrageenan injury and other treatment groups. Where, ns is non-significant, * & α represents $P < 0.05$, ** & β represents $P < 0.001$, *** & $\alpha\beta$ represents $P < 0.0001$.

Apoptosis, a well-known process of cell death (Bertheloot et al., 2021), can be accessed via annexin V (Bhatti et al., 2013) and measurement of apoptotic marker p53 (Ali et al., 2016). It was observed in this present research that NLC-loaded BMSCs lysate significantly inhibited the apoptosis of H₂O₂ pre-stimulated NIH 3T3. Based on ELISA and immunocytochemistry assays for annexin V and p53 (see Figures 3B and 4B, C), there was a shift in the

pattern of expression of p53 and annexin V from more expression in the H₂O₂ pre-stimulated NIH 3T3 to less expression in the post-treated cells significantly in NLC loaded BMSCs lysate group.

To evaluate the anti-inflammatory effect of drugs, carrageenan-induced rat hind paw oedema; a well-known experimental model to study acute inflammation (Soraya et al., 2021), was used. Based on carrageenan-induced rat paw oedema results, carrageenan induces an inflammatory reaction in the form of swelling. Maximum rat paw volume is noticed at 3 to 6 hours after induction of carrageenan in the untreated carrageenan injury group (see Figure 6), which is in accordance with the previous literature (Cong et al., 2015). NLC-loaded BMSCs lysate initiated anti-inflammatory activity at 2 hours after administration, and inflammation declined significantly compared to the untreated group, mentioned by Su et al. (2011) for flavone glycoside.

Gene expression profiling was performed to gain insight into the molecular pathways affiliated to proliferative, inflammatory, and apoptotic effects of NLC-loaded BMSCs lysate *in-vitro* in H₂O₂ pre-stimulated NIH 3T3 cells and *in-vivo* in carrageenan-induced rat paw oedema. Real-time PCR results revealed apoptotic induction was linked with increment in the expression of BAX and caspase-3 in the injury group *in-vitro* (I-H₂O₂) (see Figure 5A) and *in-vivo* (carrageenan-C and carrageenan-induced normal saline-C-NS) (see Figure 7A). In comparison, both genes expressions were significantly downregulated in NLC loaded BMSCs lysate group compared to other treatment groups. BAX is a pro-apoptotic marker involved in mitochondrial-induced cellular death by apoptosis (Westphal et al., 2011). H₂O₂ causes apoptosis by up-regulating pro-apoptotic gene expression and cleaving caspases-3 (Ma et al., 2022).

Oxidative stress causes upregulation of pro-inflammatory cytokines and activates the cell's inflammatory signal transduction pathway (Zhang et al., 2016). This causes the upregulation of pro-inflammatory cytokines; interleukin-6 (IL-6) (Liau et al., 2016) and interleukin-8 (IL-8) (Dong et al., 1998). Thus, in this present study, pro-inflammatory cytokines, IL-6 and IL-8 down-regulation were observed in post-treated NLC-loaded BMSCs lysate group significantly compared to the injury, and BMSCs lysate-treated groups *in vitro* (see Figure 5B) and *in vivo* (see Figure 7B), which are in accordance with Pomari et al. (2014).

Additionally, to find out that after injury whether cells regenerate post-treatment, evaluation of proliferative markers, proliferating cell nuclear antigen (PCNA) (Myoung et al., 2006), Topoisomerases IIa (TOP2A), and Ki-67 (Milde-Langosch et al., 2013) was done. Real-time PCR results revealed that all three proliferative genes expression was significantly up-regulated in the post-treated NLC-loaded BMSCs lysate group compared to other groups both *in vitro* (see Figure 5C) and *in vivo* (see Figure 7C). A higher TOP2A and Ki-67 indicates cellular proliferation (Strasser et al., 2000). For damaged tissue regeneration, proliferation is crucial (Ryoo and Bergmann, 2012).

5. Conclusion

Concluding the results of this study, it has been revealed that NLC-loaded BMSCs lysate might help regenerate damaged tissue to restore normal functions and possibly possess anti-inflammatory activity overall via reduction of apoptosis and enhancement of proliferation. Nonetheless, to provide a potential medicinal application of NLC-loaded BMSCs lysate for modulation of inflammatory disorders, more in-depth and advanced analysis of NLC, investigation of BMSCs lysate content, understanding of detailed molecular pathways, and large-scale animal studies/trials will be required and recommended for future studies.

References

- AFZAL, A., RAFIQUE, Z., GULZAR, A., RAUF, M. and TALAL, A., 2022. Comparison of clinical and biochemical variables between patients on twice a week dialysis regime having different residual renal function: a jack in the box. *Biological and Clinical Sciences Research Journal*, vol. 2022, no. 1. <http://dx.doi.org/10.54112/bcsrj.v2022i1.129>.
- AGHASAFARI, P., GEORGE, U. and PIDAPARTI, R., 2019. A review of inflammatory mechanism in airway diseases. *Inflammation Research*, vol. 68, no. 1, pp. 59-74. <http://dx.doi.org/10.1007/s00011-018-1191-2>. PMID:30306206.
- ALI, F., KHAN, M., KHAN, S.N. and RIAZUDDIN, S., 2016. N-Acetyl cysteine protects diabetic mouse derived mesenchymal stem cells from hydrogen-peroxide-induced injury: A novel hypothesis for autologous stem cell transplantation. *Journal of the Chinese Medical Association*, vol. 79, no. 3, pp. 122-129. <http://dx.doi.org/10.1016/j.jcma.2015.09.005>. PMID:26923123.
- ARSHAD, S., REHMAN, M., ZULFIQAR, J., NAJAM, S., ASIM, M.H. and ABID, F., 2019. Compatibility analysis of bergapten with different pharmaceutical excipients used in nanostructured lipid carriers. *Pakistan Journal of Pharmaceutical Sciences*, vol. 32, no. 6, pp. 2879-2885. PMID:32024628.
- AWAN, S.J., TARIQ, K., NASIR, G.A., BATOOL, W., SHERAZ, M.A., AHMED, S., MAQBOOL, T., ALI, U. and ANSARI, F., 2017. *Cassia fistula* seed extract enhances apoptosis in HeLa cell line via activating annexin V and p53. *Science Letters*, vol. 5, no. 1, pp. 93-104.
- BERTHELOOT, D., LATZ, E. and FRANKLIN, B.S., 2021. Necroptosis, pyroptosis and apoptosis: an intricate game of cell death. *Cellular & Molecular Immunology*, vol. 18, no. 5, pp. 1106-1121. <http://dx.doi.org/10.1038/s41423-020-00630-3>. PMID:33785842.
- BHATTI, F.-U.-R., MEHMOOD, A., WAJID, N., RAUF, M., KHAN, S.N. and RIAZUDDIN, S., 2013. Vitamin E protects chondrocytes against hydrogen peroxide-induced oxidative stress *in vitro*. *Inflammation Research*, vol. 62, no. 8, pp. 781-789. <http://dx.doi.org/10.1007/s00011-013-0635-y>. PMID:23722449.
- BUTT, S., ABBAS, U., ARSHAD, A., AHMAD, B., ASHRAF, A., HASEEB, M., BUTT, A., RANA, M. and HAFEEZ, M., 2022. Assessment of oxidative stress and inflammatory markers of medical importance in oral squamous cell carcinoma. *Biological and Clinical Sciences Research Journal*, vol. 2022, pp. 91. <http://dx.doi.org/10.54112/bcsrj.v2022i1.91>.
- CONG, H., KHAZIACHMETOVA, V.N. and ZIGASHINA, L.E., 2015. Rat paw oedema modeling and NSAIDs: timing of effects. *International Journal of Risk & Safety in Medicine*, vol. 27, Suppl. 1, pp. S76-S77. <http://dx.doi.org/10.3233/JRS-150697>. PMID:26639722.

- DONG, W., SIMEONOVA, P.P., GALLUCCI, R., MATHESON, J., FLOOD, L., WANG, S., HUBBS, A. and LUSTER, M.L., 1998. Toxic metals stimulate inflammatory cytokines in hepatocytes through oxidative stress mechanisms. *Toxicology and Applied Pharmacology*, vol. 151, no. 2, pp. 359-366. <http://dx.doi.org/10.1006/taap.1998.8481>. PMID:9707512.
- FERREIRA, K.C.B., VALLE, A.B.C.D.S., PAES, C.Q., TAVARES, G.D. and PITTELLA, F., 2021. Nanostructured lipid carriers for the formulation of topical anti-inflammatory nanomedicines based on natural substances. *Pharmaceutics*, vol. 13, no. 9, pp. 1454. <http://dx.doi.org/10.3390/pharmaceutics13091454>. PMID:34575531.
- FURMAN, D., CAMPISI, J., VERDIN, E., CARRERA-BASTOS, P., TARG, S., FRANCESCHI, C., FERRUCCI, L., GILROY, D.W., FASANO, A., MILLER, G.W., MILLER, A.H., MANTOVANI, A., WEYAND, C.M., BARZILAI, N., GORONZY, J.J., RANDO, T.A., EFFROS, R.B., LUCIA, A., KLEINSTREUER, N. and SLAVICH, G.M., 2019. Chronic inflammation in the etiology of disease across the life span. *Nature Medicine*, vol. 25, no. 12, pp. 1822-1832. <http://dx.doi.org/10.1038/s41591-019-0675-0>. PMID:31806905.
- GE, J., GUO, L., WANG, S., ZHANG, Y., CAI, T., ZHAO, R. and WU, Y., 2014. The size of mesenchymal stem cells is a significant cause of vascular obstructions and stroke. *Stem Cell Reviews and Reports*, vol. 10, no. 2, pp. 295-303. <http://dx.doi.org/10.1007/s12015-013-9492-x>.
- HOSSEN, M.J., YANG, W.S., KIM, D., ARAVINTHAN, A., KIM, J.-H. and CHO, J.Y., 2017. Thymoquinone: an IRAK1 inhibitor with in vivo and in vitro anti-inflammatory activities. *Scientific Reports*, vol. 7, no. 1, pp. 42995. <http://dx.doi.org/10.1038/srep42995>.
- HU, F.-Q., JIANG, S.P., DU, Y.Z., YUAN, H., YE, Y.Q. and ZENG, S., 2005. Preparation and characterization of stearic acid nanostructured lipid carriers by solvent diffusion method in an aqueous system. *Colloids and Surfaces. B, Biointerfaces*, vol. 45, no. 3-4, pp. 167-173. <http://dx.doi.org/10.1016/j.colsurfb.2005.08.005>. PMID:16198092.
- KIM, J.K., YUAN, H., NIE, J., YANG, Y.T., LEGGAS, M., POTTER, P.M., RINEHART, J., JAY, M. and LU, X., 2012. High payload dual therapeutic-imaging nanocarriers for triggered tumor delivery. *Small*, vol. 8, no. 18, pp. 2895-2903. <http://dx.doi.org/10.1002/smll.201200437>. PMID:2277758.
- LIAU, L.L., SUZANA, M., AZURAH, A.G.N. and CHUA, K.H., 2016. Hydrogen peroxide induces acute injury and up-regulates inflammatory gene expression in hepatocytes: an in vitro model. *Sains Malaysiana*, vol. 45, no. 3, pp. 451-458.
- MA, L., LIU, J., LIU, A. and WANG, Y., 2022. Cytoprotective effect of Selenium polysaccharide from *Pleurotus ostreatus* against H₂O₂-induced oxidative stress and apoptosis in PC12 cells. *Arabian Journal of Chemistry*, vol. 15, no. 4, pp. 103686. <http://dx.doi.org/10.1016/j.arabjc.2022.103686>.
- MALIK, A., HAFEEZ, K., NAZAR, W., NAEEM, M., ALI, I., ALI, Q., AHMED, A., MUJTABA, Z., RANA, M. and HAFEEZ, M., 2021. Assessment of controversial risk factors in development of breast cancer: a study from local population. *Biological and Clinical Sciences Research Journal*, vol. 2020, pp. 49. <http://dx.doi.org/10.54112/bcsrj.v2021i1.49>.
- MALIK, S. and MALIK, T., 2021. Mesenchymal stem cells lysate as a cell-free therapy: a review. *Current Biotechnology*, vol. 10, no. 2, pp. 78-87. <http://dx.doi.org/10.2174/2211550110666210617093954>.
- MASGUTOV, R., ZEINALOVA, A., BOGOV, A., MASGUTOVA, G., SALAFUTDINOV, I., GARANINA, E., SYROMIATNIKOVA, V., IDRISOVA, K., MULLAKHMETOVA, A., ANDREEVA, D., MUKHAMETOVA, L., KADYROV, A., PANKOV, I. and RIZVANOV, A., 2021. Angiogenesis and nerve regeneration induced by local administration of plasmid pBud-coVEGF165-coFGF2 into the intact rat sciatic nerve. *Neural Regeneration Research*, vol. 16, no. 9, pp. 1882-1889. <http://dx.doi.org/10.4103/1673-5374.306090>. PMID:33510097.
- MILDE-LANGOSCH, K., KARN, T., MÜLLER, V., WITZEL, I., RODY, A., SCHMIDT, M. and WIRTZ, R.M., 2013. Validity of the proliferation markers Ki67, TOP2A, and RacGAP1 in molecular subgroups of breast cancer. *Breast Cancer Research and Treatment*, vol. 137, no. 1, pp. 57-67. <http://dx.doi.org/10.1007/s10549-012-2296-x>. PMID:23135572.
- MOCCIA, F., NEGRI, S., SHEKHA, M., FARIS, P. and GUERRA, G., 2019. Endothelial Ca²⁺ signaling, angiogenesis and vasculogenesis: just what it takes to make a blood vessel. *International Journal of Molecular Sciences*, vol. 20, no. 16, pp. 3962. <http://dx.doi.org/10.3390/ijms20163962>. PMID:31416282.
- MOHANTY, A., POLISETTI, N. and VEMUGANTI, G.K., 2020. Immunomodulatory properties of bone marrow mesenchymal stem cells. *Journal of Biosciences*, vol. 45, no. 1, pp. 1-17. <http://dx.doi.org/10.1007/s12038-020-00068-9>. PMID:32713861.
- MYOUNG, H., KIM, M.J., LEE, J.H., OK, Y.J., PAENG, J.Y. and YUN, P.Y., 2006. Correlation of proliferative markers (Ki-67 and PCNA) with survival and lymph node metastasis in oral squamous cell carcinoma: a clinical and histopathological analysis of 113 patients. *International Journal of Oral and Maxillofacial Surgery*, vol. 35, no. 11, pp. 1005-1010. <http://dx.doi.org/10.1016/j.ijom.2006.07.016>. PMID:17018251.
- NOOR, S., HAYAT, S., HUSSAIN, M., MAHMOOD, S., PERVAIZ, S., HANIF, S. and RANA, M., 2022. Effects of vitamin c and e on lipid profile and kidney performance of albino rats. *Biological and Clinical Sciences Research Journal*, vol. 2022, no. 1. <http://dx.doi.org/10.54112/bcsrj.v2022i1.87>.
- POMARI, E., STEFANON, B. and COLITTI, M., 2014. Effect of plant extracts on H2O2-induced inflammatory gene expression in macrophages. *Journal of Inflammation Research*, vol. 7, pp. 103-112. PMID:25075197.
- RYOO, H.D. and BERGMANN, A., 2012. The role of apoptosis-induced proliferation for regeneration and cancer. *Cold Spring Harbor Perspectives in Biology*, vol. 4, no. 8, pp. a008797. <http://dx.doi.org/10.1101/cshperspect.a008797>. PMID:22855725.
- SHARIF, S., NAKAGAWA, T., OHNO, T., MATSUMOTO, M., KITA, T., RIAZUDDIN, S. and ITO, J., 2007. The potential use of bone marrow stromal cells for cochlear cell therapy. *Neuroreport*, vol. 18, no. 4, pp. 351-354. <http://dx.doi.org/10.1097/WNR.0b013e3280287a9a>.
- SORAYA, H., AZARBAJANI, M. and KIAN, M., 2021. Anti-inflammatory effects of memantine in carrageenan-induced paw edema model in rats. *Journal of Reports in Pharmaceutical Sciences*, vol. 10, no. 1, pp. 60. http://dx.doi.org/10.4103/jrptps.JRPTPS_37_20.
- STRASSER, A., O'CONNOR, L. and DIXIT, V.M., 2000. Apoptosis signaling. *Annual Review of Biochemistry*, vol. 69, no. 1, pp. 217-245. <http://dx.doi.org/10.1146/annurev.biochem.69.1.217>. PMID:10966458.
- SU, J.-Y., LI, Q.-C. and ZHU, L., 2011. Evaluation of the in vivo anti-inflammatory activity of a flavone glycoside from *Cancrinia discoides* (Ledeb.) Poljak. *Experimental and Clinical Sciences*, vol. 10, pp. 110.
- WAJID, N., MEHMOOD, A., BHATTI, F.U., KHAN, S.N. and RIAZUDDIN, S., 2013. Lovastatin protects chondrocytes derived from Wharton's jelly of human cord against hydrogen-peroxide-induced in vitro injury. *Cell and Tissue Research*, vol. 351, no. 3, pp. 433-443. <http://dx.doi.org/10.1007/s00441-012-1540-3>. PMID:23271636.
- WAJID, N., NASEEM, R., ANWAR, S.S., AWAN, S.J., ALI, M., JAVED, S. and ALI, F., 2015. The effect of gestational diabetes on proliferation

- capacity and viability of human umbilical cord-derived stromal cells. *Cell and Tissue Banking*, vol. 16, no. 3, pp. 389-397. <http://dx.doi.org/10.1007/s10561-014-9483-4>. PMID:25407535.
- WESTPHAL, D., DEWSON, G., CZABOTAR, P.E. and KLUCK, R.M., 2011. Molecular biology of Bax and Bak activation and action. *Biochimica et Biophysica Acta. Molecular Cell Research*, vol. 1813, no. 4, pp. 521-531. <http://dx.doi.org/10.1016/j.bbamcr.2010.12.019>.
- WINTER, C.A., RISLEY, E.A. and NUSS, G.W., 1962. Carrageenin-induced edema in hind paw of the rat as an assay for antiinflammatory drugs. *Experimental Biology and Medicine*, vol. 111, no. 3, pp. 544-547. <http://dx.doi.org/10.3181/00379727-111-27849>.
- YEGHIAZARIANS, Y., ZHANG, Y., PRASAD, M., SHIH, H., SAINI, S.A., TAKAGAWA, J., SIEVERS, R.E., WONG, M.L., KAPASI, N.K., MIRSKY, R., KOSKENVUO, J., MINASI, P., YE, J., VISWANATHAN, M.N., ANGELI, F.S., BOYLE, A.J., SPRINGER, M.L. and GROSSMAN, W., 2009. Injection of bone marrow cell extract into infarcted hearts results in functional improvement comparable to intact cell therapy. *Molecular Therapy*, vol. 17, no. 7, pp. 1250-1256. <http://dx.doi.org/10.1038/mt.2009.85>. PMID:19384293.
- YOON, G., PARK, J.W. and YOON, I.-S., 2013. Solid lipid nanoparticles (SLNs) and nanostructured lipid carriers (NLCs): recent advances in drug delivery. *Journal of Pharmaceutical Investigation*, vol. 43, no. 5, pp. 353-362. <http://dx.doi.org/10.1007/s40005-013-0087-y>.
- ZAFAR, I., SAMAD, A., HAROON, A., FAYYAZ, N., FAYYAZ, N., MAHMOOD, N. and BUKHARI, A., 2022. Correlation between fine needle aspiration cytology and corresponding ultrasound birads score in mammary malignancy. *Biological and Clinical Sciences Research Journal*, vol. 2022, no. 1. <http://dx.doi.org/10.54112/bcsrj.v2022i1.130>.
- ZHANG, H., LIU, R. and TSAO, R., 2016. Anthocyanin-rich phenolic extracts of purple root vegetables inhibit pro-inflammatory cytokines induced by H₂O₂ and enhance antioxidant enzyme activities in Caco-2 cells. *Journal of Functional Foods*, vol. 22, pp. 363-375. <http://dx.doi.org/10.1016/j.jff.2016.01.004>.

Supplementary Material

Supplementary material accompanies this paper.

Supplementary Information. The details of materials and methods and in-vivo results pictures have been provided in the supplementary information.

This material is available as part of the online article from <https://doi.org/10.1590/1519-6984.269553>